



Energy partition and segregation for an intruder in a vibrated granular system under gravity

J. Javier Brey

Física Teórica, Universidad de Sevilla, Spain

M.J. Ruiz-Montero

F. Moreno

UCSB, May 2005

Introduction

Two observed peculiarities of vibrated granular systems:

- Breakdown of energy equipartition \Leftrightarrow different species have different granular temperatures

R.D. Wildman and D.J. Parker, Phys. Rev. Lett. **88**, 064301 (2002); K. Feitosa and N. Menon, Phys. Rev. Lett. **88**, 198301 (2002)

Introduction

Two observed peculiarities of vibrated granular systems:

- **Breakdown of energy equipartition** \Leftrightarrow different species have different granular temperatures

R.D. Wildman and D.J. Parker, Phys. Rev. Lett. **88**, 064301 (2002); K. Feitosa and N. Menon, Phys. Rev. Lett. **88**, 198301 (2002)

- **Particle segregation** \Leftrightarrow demix of a mixture when shaken

J. Duran, J. Rajchenbach, and E. Clément, Phys. Rev. Lett. **70**, 2431 (1993); A.P.J. Breu, H.-M. Ensner, C.A. Kruelle, and I. Rehberg, Phys. Rev. Lett. **90**, 014302 (2003)

Introduction

Two observed peculiarities of vibrated granular systems:

- **Breakdown of energy equipartition** \Leftrightarrow different species have different granular temperatures

R.D. Wildman and D.J. Parker, Phys. Rev. Lett. **88**, 064301 (2002); K. Feitosa and N. Menon, Phys. Rev. Lett. **88**, 198301 (2002)

- **Particle segregation** \Leftrightarrow demix of a mixture when shaken

J. Duran, J. Rajchenbach, and E. Clément, Phys. Rev. Lett. **70**, 2431 (1993); A.P.J. Breu, H.-M. Ensner, C.A. Kruelle, and I. Rehberg, Phys. Rev. Lett. **90**, 014302 (2003)

- Both effects will be investigated here for a dilute mixture in the tracer limit by means of kinetic theory. It will be shown that there is a close relationship between them

The system

- Low density gas of inelastic hard disks ($d = 2$) or spheres ($d = 3$) of mass m and diameter σ . Coefficient of normal restitution: α

The system

- Low density gas of inelastic hard disks ($d = 2$) or spheres ($d = 3$) of mass m and diameter σ . Coefficient of normal restitution: α
- Plus, one impurity/intruder (tracer limit) of mass m_0 and diameter σ_0 . Coefficient of normal restitution fluid-intruder: α_0

The system

- Low density gas of inelastic hard disks ($d = 2$) or spheres ($d = 3$) of mass m and diameter σ . Coefficient of normal restitution: α
- Plus, one impurity/intruder (tracer limit) of mass m_0 and diameter σ_0 . Coefficient of normal restitution fluid-intruder: α_0
- Uniform gravitational external field of intensity g_0

The system

- Low density gas of inelastic hard disks ($d = 2$) or spheres ($d = 3$) of mass m and diameter σ . Coefficient of normal restitution: α
- Plus, one impurity/intruder (tracer limit) of mass m_0 and diameter σ_0 . Coefficient of normal restitution fluid-intruder: α_0
- Uniform gravitational external field of intensity g_0
- The bottom wall, located at $z = 0$, is vibrating with small amplitude and high frequency. There is no upper wall

The system

- Low density gas of inelastic hard disks ($d = 2$) or spheres ($d = 3$) of mass m and diameter σ . Coefficient of normal restitution: α
- Plus, one impurity/intruder (tracer limit) of mass m_0 and diameter σ_0 . Coefficient of normal restitution fluid-intruder: α_0
- Uniform gravitational external field of intensity g_0
- The bottom wall, located at $z = 0$, is vibrating with small amplitude and high frequency. There is no upper wall
- The system exhibits an inhomogeneous steady state with gradients only in the direction of the external field (Huntley's talk). The hydrodynamic profiles are not affected by the presence of the impurity

Temperature profiles

- $T(z)$ and $T_0(z)$ are defined in the usual way from the average kinetic energies

Temperature profiles

- $T(z)$ and $T_0(z)$ are defined in the usual way from the average kinetic energies
- **Assuming** there is a hydrodynamic regime for the impurity **and** that the associated 'normal solution' of the Boltzmann equation can be generated by the Chapman-Enskog procedure \Rightarrow

$$\zeta^{(0)}(z) = \zeta_0^{(0)}(z)$$

\longrightarrow Local Homogenous Cooling Rates for the fluid and the intruder are the same

Temperature profiles

- $T(z)$ and $T_0(z)$ are defined in the usual way from the average kinetic energies
- **Assuming** there is a hydrodynamic regime for the impurity **and** that the associated 'normal solution' of the Boltzmann equation can be generated by the Chapman-Enskog procedure \Rightarrow

$$\zeta^{(0)}(z) = \zeta_0^{(0)}(z)$$

\longrightarrow Local Homogenous Cooling Rates for the fluid and the intruder are the same

- **This is not a small gradient approximation**, but valid to all orders in the gradients. Even more, it holds for any hydrodynamic state of the fluid

Temperature profiles

- $T(z)$ and $T_0(z)$ are defined in the usual way from the average kinetic energies
- **Assuming** there is a hydrodynamic regime for the impurity **and** that the associated 'normal solution' of the Boltzmann equation can be generated by the Chapman-Enskog procedure \Rightarrow

$$\zeta^{(0)}(z) = \zeta_0^{(0)}(z)$$

\longrightarrow Local Homogenous Cooling Rates for the fluid and the intruder are the same

- **This is not a small gradient approximation**, but valid to all orders in the gradients. Even more, it holds for any hydrodynamic state of the fluid
- $\zeta^{(0)}$ and $\zeta_0^{(0)}$ are functional of the distribution functions. A good approximation for them is obtained by using Maxwellians*

- In this way, it is obtained

$$(1 + \phi)^{1/2} \left(1 - h \frac{1 + \phi}{\phi} \right) = \frac{\beta}{h}$$

$$\phi = \frac{mT_0(z)}{m_0T(z)} \quad h \equiv \frac{m(1 + \alpha_0)}{2(m + m_0)} \quad \beta \equiv \frac{1 - \alpha^2}{4\sqrt{2}} \left(\frac{\sigma}{\bar{\sigma}} \right)^{d-1}$$

with $\bar{\sigma} \equiv (\sigma + \sigma_0)/2$

- In this way, it is obtained

$$(1 + \phi)^{1/2} \left(1 - h \frac{1 + \phi}{\phi} \right) = \frac{\beta}{h}$$

$$\phi = \frac{mT_0(z)}{m_0T(z)} \quad h \equiv \frac{m(1 + \alpha_0)}{2(m + m_0)} \quad \beta \equiv \frac{1 - \alpha^2}{4\sqrt{2}} \left(\frac{\sigma}{\bar{\sigma}} \right)^{d-1}$$

with $\bar{\sigma} \equiv (\sigma + \sigma_0)/2$

- Cubic equation for ϕ , with a unique real solution for all the physical values of h and ϕ

- In this way, it is obtained

$$(1 + \phi)^{1/2} \left(1 - h \frac{1 + \phi}{\phi} \right) = \frac{\beta}{h}$$

$$\phi = \frac{mT_0(z)}{m_0T(z)} \quad h \equiv \frac{m(1 + \alpha_0)}{2(m + m_0)} \quad \beta \equiv \frac{1 - \alpha^2}{4\sqrt{2}} \left(\frac{\sigma}{\bar{\sigma}} \right)^{d-1}$$

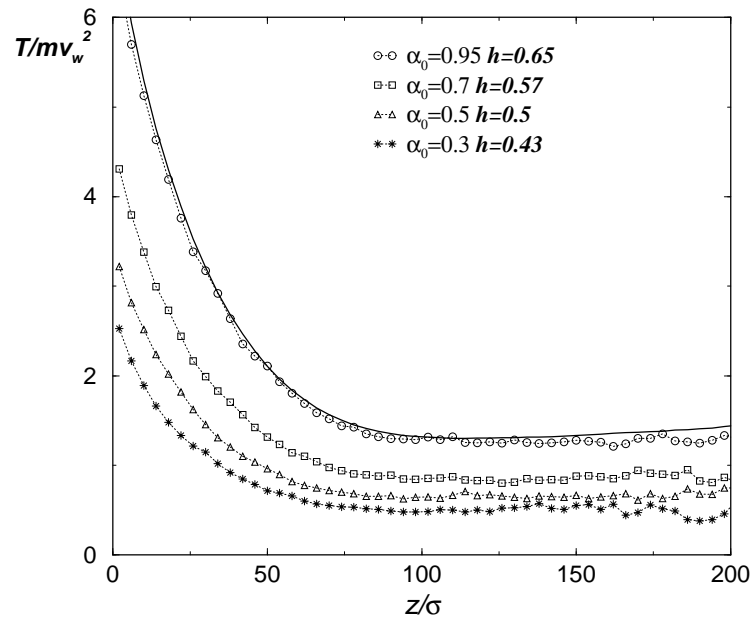
with $\bar{\sigma} \equiv (\sigma + \sigma_0)/2$

- Cubic equation for ϕ , with a unique real solution for all the physical values of h and ϕ
- $\Rightarrow \phi$ does not depend on z (Feitosa and Menon, 2002), but it strongly depends on the inelasticity. Outside the tracer limit, also densities dependence

MD simulations I. Temperature profiles

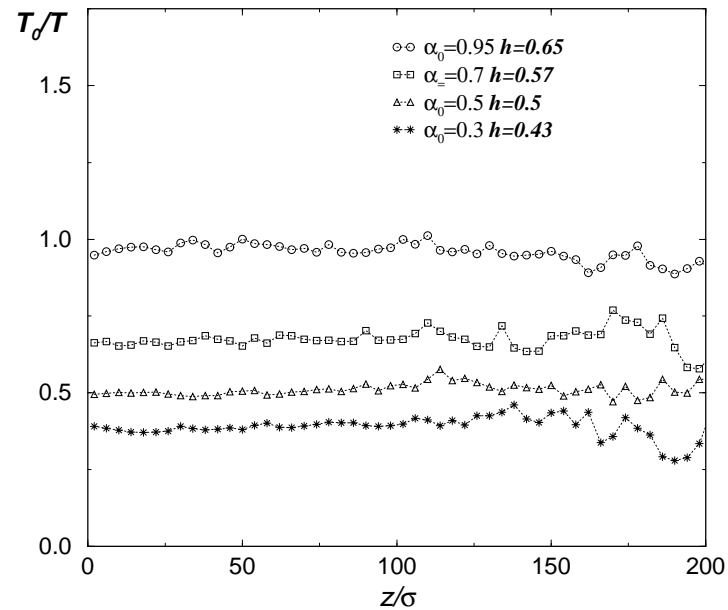
- $d = 2$, $N = 359$, $\alpha = 0.95$, $\sigma_0 = \sigma$, S (width) = 50σ , wall moves in a sawtooth way with $v_w = 5(\sigma g)^{1/2}$

- $\frac{m_0}{m} = \frac{1}{2}$



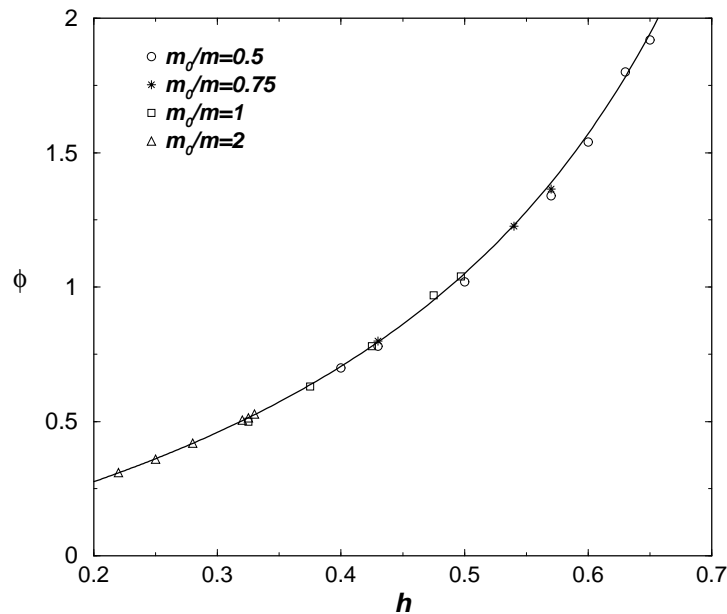
MD simulations II. Profiles of the temperature ratio

- Same values of the parameters as in the previous figure



Similar behavior for $m_0/m = 0.75, 1, 2$

MD simulations III. Comparison with the theoretical predictions



- ϕ can be larger than unity even if $m/m_0 < 1$, and viceversa

(more)

Impurity density $n_0(z)$

- In the steady state the associated flux j_z must vanish

Impurity density $n_0(z)$

- In the steady state the associated flux j_z must vanish
- To first order in the gradients, Chapman-Enskog gives

$$j_z = -m_0 D \partial_z x_0 - \frac{mn}{T(z)} D' \partial_z T - \frac{m}{T(z)} D_p \partial_z p(z)$$

with $x_0 \equiv n_0/n$, $p = nT$, D = diffusion coefficient, D' = thermal diffusion coefficient, D_p = pressure diffusion coefficient

$$D_p = \frac{n_0 T_0 \phi - 1}{mn \phi} \left(\nu - \frac{3\zeta^{(0)}}{2} + \frac{\zeta^{(0)2}}{2\nu} \right)^{-1} \quad \phi = \frac{mT_0(z)}{m_0 T(z)}$$

ν = some collision frequency (*)

- The position (maximum density or center of mass) of the intruder relative to the fluid is determined by the sign of D_p . Similar to the elastic case (barometric formule), where $\phi = \frac{m}{m_0}$

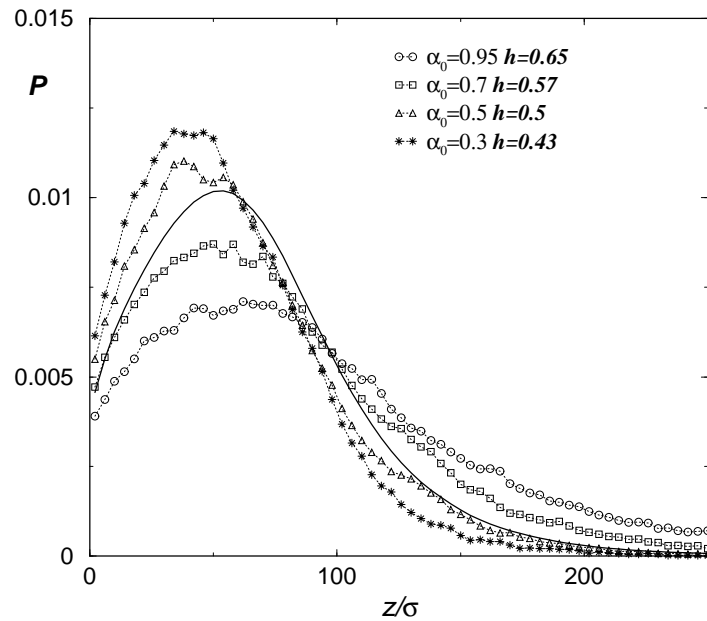
- The position (maximum density or center of mass) of the intruder relative to the fluid is determined by the sign of D_p . Similar to the elastic case (barometric formule), where $\phi = \frac{m}{m_0}$
- \longrightarrow segregation criterium for this particular case

- The position (maximum density or center of mass) of the intruder relative to the fluid is determined by the sign of D_p . Similar to the elastic case (barometric formule), where $\phi = \frac{m}{m_0}$
- \longrightarrow segregation criterium for this particular case
- General discussion quite complicated, but in a wide parameter region, defined by $\beta < h/2$, the sign of D_p is determined by the value of ϕ

- The position (maximum density or center of mass) of the intruder relative to the fluid is determined by the sign of D_p . Similar to the elastic case (barometric formule), where $\phi = \frac{m}{m_0}$
- \longrightarrow segregation criterium for this particular case
- General discussion quite complicated, but in a wide parameter region, defined by $\beta < h/2$, the sign of D_p is determined by the value of ϕ
- -For $\phi > 1$, the impurity position is 'higher' than that of the gas
- -For $\phi < 1$, the impurity position is 'lower' than that of the gas

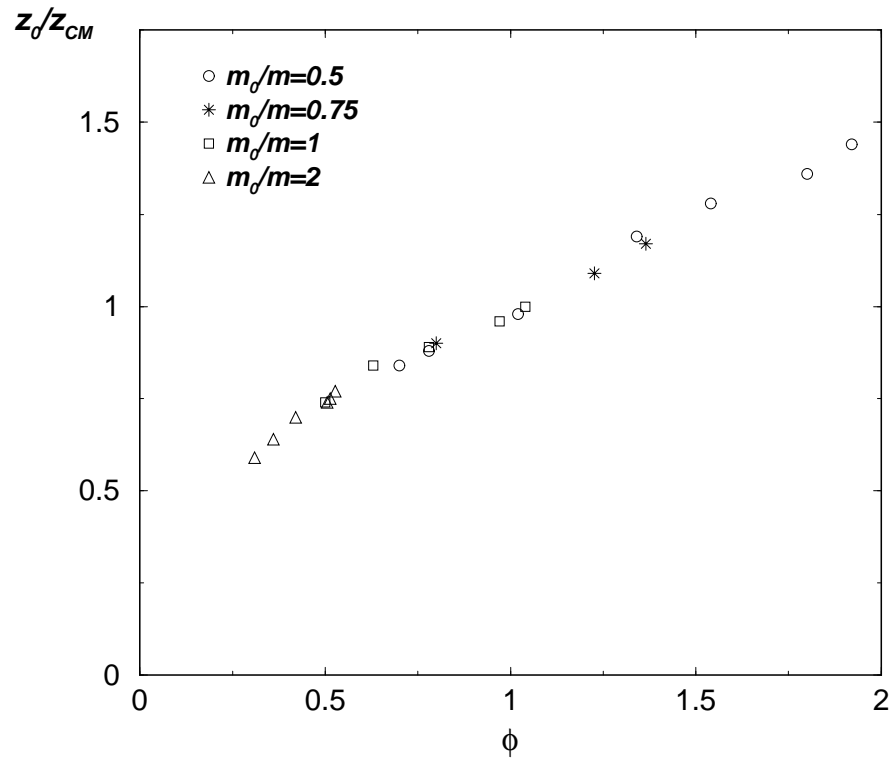
MD simulations IV. Normalized density profiles

$$m_0/m = 1/2, \alpha = 0.95$$



Qualitative agreement with theory (ϕ increases as α_0 increases)

MD simulations V. Ratio of the center of mass positions



(more)

Some additional comments

- The analysis of the ratio of the temperatures in a mixture can be easily extended beyond the tracer limit and also to high densities (keeping the Maxwellian approximation)

Some additional comments

- The analysis of the ratio of the temperatures in a mixture can be easily extended beyond the tracer limit and also to high densities (keeping the Maxwellian approximation)
- The segregation criterium is also easily extended beyond the tracer limit, but it seems hard to extend to high densities, since explicit expressions of mass transport coefficients are needed (Enskog theory?)

Some additional comments

- The analysis of the ratio of the temperatures in a mixture can be easily extended beyond the tracer limit and also to high densities (keeping the Maxwellian approximation)
- The segregation criterium is also easily extended beyond the tracer limit, but it seems hard to extend to high densities, since explicit expressions of mass transport coefficients are needed (Enskog theory?)
- Moreover, at high density, other effects also leading to segregation may become relevant, as for instance those discussed in: D.C. Hong, P.V. Quinn, and S. Luding, Phys. Rev. Lett. **86**, 3423 (2001); J.T. Jenkins and D.K. Yoon, Phys. Rev. Lett. **88**, 194301 (2002)

Some additional comments

- The analysis of the ratio of the temperatures in a mixture can be easily extended beyond the tracer limit and also to high densities (keeping the Maxwellian approximation)
- The segregation criterium is also easily extended beyond the tracer limit, but it seems hard to extend to high densities, since explicit expressions of mass transport coefficients are needed (Enskog theory?)
- Moreover, at high density, other effects also leading to segregation may become relevant, as for instance those discussed in: D.C. Hong, P.V. Quinn, and S. Luding, Phys. Rev. Lett. **86**, 3423 (2001); J.T. Jenkins and D.K. Yoon, Phys. Rev. Lett. **88**, 194301 (2002)
- On the other hand, there is no reason to expect that the mechanism discussed here be no important at high densities

The local HCS cooling rates in the Maxwellian approximation

$$\zeta^{(0)*} \equiv \frac{\zeta^{(0)}(z)}{n(z)\sigma^{d-1}v_g(z)} = \frac{\sqrt{2}\pi^{(d-1)/2}}{\Gamma(d/2)d} (1 - \alpha^2)$$

$$\zeta_0^{(0)*} \equiv \frac{\zeta_0^{(0)}(z)}{n(z)\sigma^{d-1}v_g(z)} = \nu_0^*(1 + \phi)^{1/2} \left(1 - h\frac{1 + \phi}{\phi}\right)$$

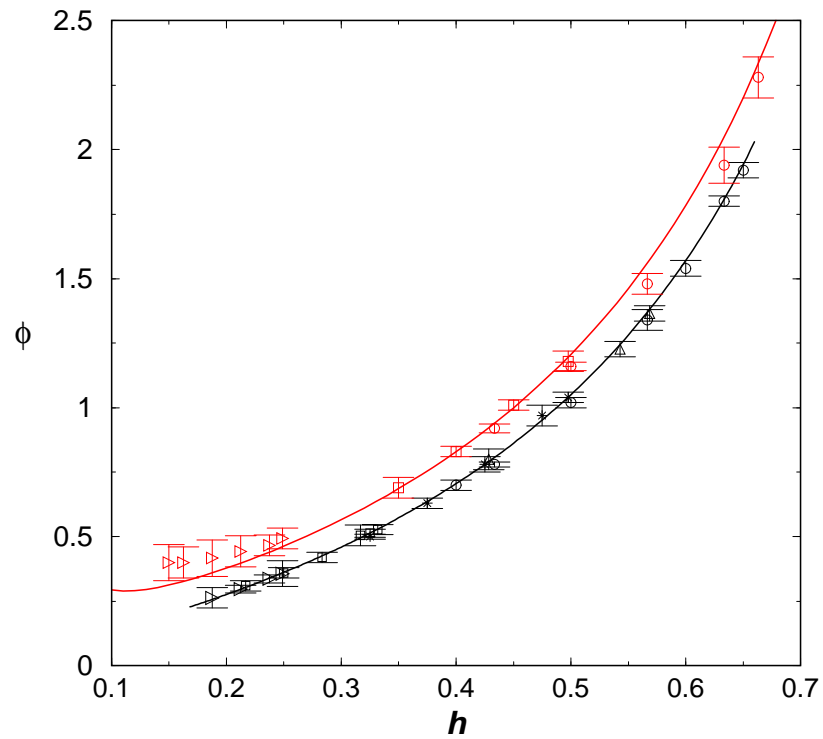
where $n(z)$ is the number density of the gas,

$$v_g(z) = \left[\frac{2T(z)}{m}\right]^{1/2} \quad h = \frac{m(1 + \alpha_0)}{2(m + m_0)} \quad \nu_0^* = \frac{8h\pi^{(d-1)/2}}{\Gamma(d/2)d} \left(\frac{\bar{\sigma}}{\sigma}\right)^{d-1}$$

$$\bar{\sigma} = \frac{\sigma + \sigma_0}{2} \quad \phi = \frac{mT_0(z)}{m_0T(z)}.$$

(back)

MD simulations IIIa. Comparison with theory



- black symbols $\alpha = 0.95$

- red symbols $\alpha = 0.8$

(back)

Diffusion coefficients

$$D = \frac{nT_0}{m_0} \left(\nu - \frac{\zeta^{(0)}}{2} \right)^{-1} \quad D' = -\frac{\zeta^{(0)}}{2\nu} D_p$$

$$D_p = \frac{n_0 T_0 \phi - 1}{mn \phi} \left(\nu - \frac{3\zeta^{(0)}}{2} + \frac{\zeta^{(0)2}}{2\nu} \right)^{-1}$$

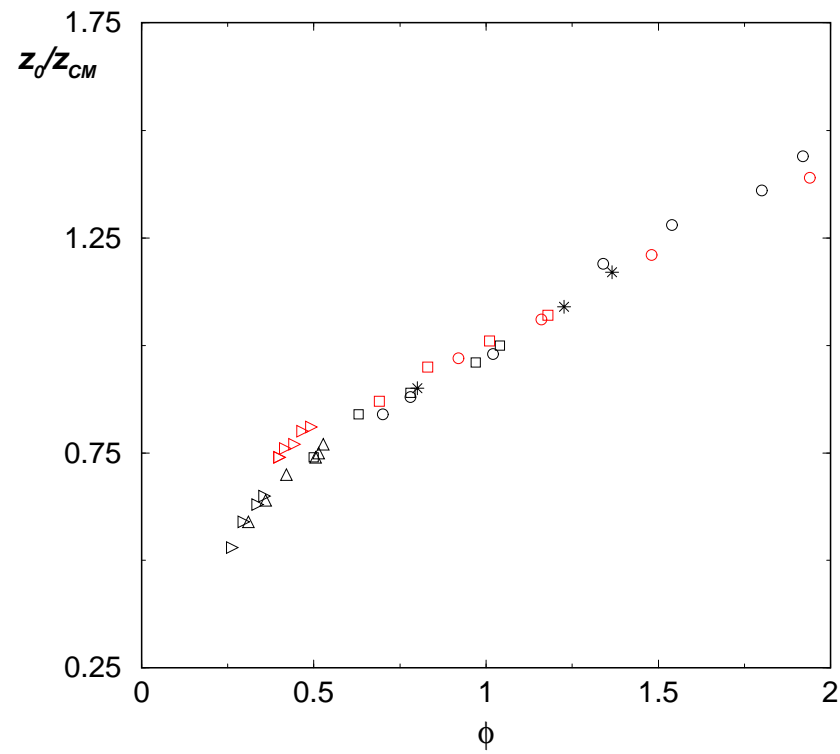
Here,

$$\nu = \nu_e \frac{1 + \alpha}{2} (1 - \Delta)^{1/2} (1 + \phi)^{1/2}$$

$$\Delta = \frac{m}{m + m_0} \quad \nu_e = \frac{4\sqrt{2}\pi^{(d-1)/2}}{\Gamma(d/2)d} \bar{\sigma}^{d-1} \Delta^{1/2} n \left(\frac{T}{m_0} \right)^{1/2}$$

(back)

MD simulations Va. Ratio of the center of mass positions



- black symbols $\alpha = 0.95$

- red symbols $\alpha = 0.8$

(back)